Hyperfine splittings of hydrogenlike ions and the dynamic-correlation model for one-hole nuclei

M. Tomaselli,[1] T. Kühl,[2] P. Seelig,[2] C. Holbrow,[3] and E. Kankeleit[1]

[1]*Institut für Kernphysik, Technische Universität Darmstadt, Schlossgartenstrasse 9, D-64289 Darmstadt, Germany*
[2]*Gesellschaft für Schwerionenforschung (GSI), Plankstrasse 1, D-64291 Darmstadt, Germany*
[3]*Colgate University, Hamilton, New York 13346*

The dynamic-correlation model (DCM) has been used to calculate the ground-state hyperfine splitting in hydrogenlike ions characterized by core nuclei with one valence neutron or proton hole. For such nuclei the DCM nonperturbatively couples the single hole to the collective states of the reference closed-shell core. Within this nuclear model the magnetic moments, the nuclear radii, and the quadrupole moments of the ground states are well reproduced. The hyperfine splittings of ^{165}Ho^{66+}, ^{185}Re^{74+}, ^{187}Re^{74+}, and ^{207}Pb^{81+} are calculated from the derived configuration-mixing amplitudes. In all cases a very good agreement with measured values is obtained. [S0556-2813(98)02709-5]

PACS number(s): 21.60.−n, 21.10.−k, 27.70.+q, 32.10.Fn

I. INTRODUCTION

The hyperfine splitting of hydrogenlike ions with nuclei possessing one valence neutron (proton) hole is investigated by using the dynamic correlation model (DCM). The DCM has already been successfully applied [1] to describe the ground-state hyperfine splitting of the one-valence-particle nucleus ^{209}Bi. With the DCM model we calculate the ground-state amplitudes of the valence hole strongly mixed with dynamic correlated states. These result from vector coupling the valence hole with the collective excitations of the reference core. Using these amplitudes we evaluate the magnetic moments, the quadrupole moments, and the nuclear radii of the ground states of the nuclei under investigation. The magnetic moments of such nuclei deviate from the Schmidt values predicted by the single-hole shell model. The deviation is small for the ^{207}Pb ground state and much larger in the other cases. Therefore the DCM has the challenging task of reproducing extremely different magnitudes of corrections to the shell model.

For the sake of comparison it is useful to summarize some of the other models used to calculate the distribution of magnetization in nuclei.

A first modification of the single-hole description of a hole nucleus $(A−1)$ is to allow the single hole to interact as a small perturbation with the residual core. Perturbation calculations which introduce the core-polarization diagrams within spin-flip excitations were performed as early as in Ref. [2].

In Ref. [3] the core-polarization calculations were extended to include the effects of the nuclear medium. With this approximation there is still a small discrepancy between the theoretical and measured magnetic moments. This is thought to be due to the need to correct the gyromagnetic ratios for the effect of "quenching" arising from the appearance of the meson degrees of freedom in the nuclear-structure calculation [4].

Reference [5] presents first- and second-order polarization calculations performed for nuclei in the Pb region with a quenched gyromagnetic factor. The analysis is in terms of g_l, g_s, and g_p and takes into account (i) core polarization,

(ii) two body *LS* force, (iii) meson exchange current, and (iv) higher-order configuration mixing in the the nuclear wave functions. The results reported in Ref. [5] show that perturbation calculations with the quenching of the gyromagnetic factor g_l and the introduction of g_p reproduce the magnetic moment of the neutron-hole ground state of ^{207}Pb reasonably well, but they fail for the proton-hole ground state of ^{165}Ho. No calculations were performed in Ref. [5] for the rhenium isotopes.

In this paper we apply the nonperturbative DCM of Ref. [6] to calculate the nuclear ground-state properties of the one hole nuclei ^{165}Ho, ^{185}Re, ^{186}Re, and ^{207}Pb. This approach provides a consistent treatment of the core polarization and of the "quenching factor" in a dynamic approximation. In various numerical applications [7,8] good agreement has been achieved between the calculated and the measured magnetic properties of light and heavy nuclei. The theoretical calculations were performed using exact factorization methods which simplify the computation of the many-body matrix elements of the model operators in the dynamic correlated basis.

The correlated dynamics are generated in this case by the residual interaction between the valence proton or neutron hole and the particles of the model vacuum, which leads to to the formation of the model configuration mixing wave functions (CMWFs). In this paper the CMWFs are obtained by allowing the valence $2d_{5/2}$, $2f_{7/2}$ proton hole, and the $3p_{1/2}$ neutron hole to polarize the core via proton and neutron particle-hole excitations $(2\hbar\omega)$. This structure of the closed-shell vacuum state modifies the valence-hole configuration space and introduces into the model space (a) closed-shell polarization of normal parity and (b) closed-shell polarization of non-normal-parity. These states have the same quantum numbers as the low-energy mesons $(\omega, \rho, \dots)$ and are characterized, in this nonperturbative approximation, by many particle-hole pairs mixed via the two-body interaction with the valence state.

As we discuss in Sec. IV, the amplitudes of these modes, calculated with a specific choice of the single-particle energies and the two-body potential, contribute coherently as in Ref. [1] to the formation of the magnetic distributions of

[165]Ho, [185]Re, [186]Re, and [207]Pb. If we associate this coherent effect with the degree of collectivity of the model, these non-normal-parity polarizations are very well represented in the present calculations by collective states that bear the quantum numbers of the low-energy mesons. On this assumption, we include in the calculation of the magnetic structure of nuclei both the core polarizations and the quenching (meson) effects within the same formalism. The nonlinear terms modify the structure of the single-particle operators and generate effective operators that, via the two-body current, describe the exchange of virtual mesons between two nucleons in the nuclear system.

The model has been applied to calculate ground-state wave functions which describe the magnetic and the electric properties of [165]Ho, [185]Re, [186]Re, and [207]Pb. The calculated rms radii and the nuclear charge distributions [9] are in very good agreement with the experimental values.

Our calculations can be further tested by using the model nuclear magnetization distribution to calculate the hyperfine-structure splitting of a hydrogenlike ions in the Pb region and to compare the theoretical results with the recently measured experimental values [10–13]. As we will show in Sec. III, almost perfect agreement with the experimental values has been obtained for the ground-state hyperfine splittings of the four nuclei if no radiative corrections are made. In order to understand this surprising result, already noted in Ref. [1], we present a direct comparison between the DCM calculation and the single-particle calculation of Bohr and Weisskopf [14], and we analyze the three terms generated by the DCM which contribute to the formation of the hyperfine splitting. The results presented in Table I show that the single-particle contribution of the DCM has to be associated with the term $\{\epsilon\}$ as described in Ref. [14], which in the literature is referred to as the Bohr-Weisskopf effect. The other two terms in the DCM model that characterize the magnetic splitting do not appear in the calculations of Ref.

[14]. The central question is therefore how to compare these additional terms and the radiative corrections of Ref. [15]. From the results achieved in the present calculations, we conclude that these terms have the same physical interpretation as the QED corrections if we consider the possible decay of the virtual mesons included in the nuclear structure calculations. In the following sections we modify the DCM of Ref. [1] in order to treat the $(A-1)$ nuclei.

II. MIXING OF ONE HOLE TO THE DYNAMIC CORRELATIONS (CMWFs)

The electromagnetic properties of the ground state of nuclei characterized by open shells are investigated within the DCM of Ref. [6]. The model describes the strong coupling of the single hole to the intrinsic-core states (valence coupled to the collective excitations of the reference core) within a dynamic approximation. The coupling is implemented by the residual interaction between the valence hole and the core particles which causes the deformation of the nuclear core and introduces meson effects into the structure calculations. The effect of the extended nuclear core is included in the present calculation with the help of the nonlinear equation-of-motion method, which properly linearized allows us to calculate the eigenvalue equations of the model. In this paper the hierarchy of the configuration-mixing wave functions is truncated within a dynamic-linearization approximation [6] so as to include in the calculation only the CMWFs of the first $(2h-1p)$ active states which result from the vector coupling of the valence hole with the $1p-1h$ core excitations. The higher order CMWFs $(3h-2p)$ have been linearized [16] to generate the dynamic eigenvalue equations of the model. According to this linearization approximation, the ground-state wave function $\{\phi_{j-m}\}$ of the $|A-1\rangle$ nucleus is given by

$$|\phi_{j-m}\rangle = \left[\chi_{jj}^0 a_{j-m} + \sum_{j_1 j_2 j_3 J_1} \chi_{j_1 j_2 j_3 J_1 j}^1 N_{j_1 j_2 j_3 J_1 j}^1 A_1(j_1(j_2 j_3)J_1; j-m)\right]|0\rangle$$

$$= \left[\chi_{\alpha_0 j}^0 a_{j-m} + \sum_{\alpha_1 J_1} \chi_{\alpha_1 J_1 j}^1 N_{\alpha_1 J_1 j}^1 A_1(\alpha_1 J_1; j-m)\right]|0\rangle, \tag{2.1}$$

where the operator a_{j-m} creates a single valence hole with quantum numbers $\{j^{-1}, -m\}$ and where the operator

$$A_1(\alpha_1 J_1; j-m) = A_1[j_1(j_2 j_3)J_1; j-m] = \sum_{m's} [a_{j_1} \otimes (a_{j_2}^\dagger \otimes a_{j_3})^{J_1}]_{-m}^j$$

creates the $2h$-$1p$ states, obtained, as indicated by the notation $[a_{j_1} \otimes (a_{j_2}^\dagger \otimes a_{j_3})^{J_1}]_{-m}^j$, by coupling the valence hole with quantum number $\{j_1^{-1}\}$ to the particle-hole pair with quantum numbers $\{j_2\}$ and $\{j_3^{-1}\}$, respectively. To simplify the notation we have introduced the short notations $\{\alpha_0\}$ for the $\{j\}$ quantum number and $\{\alpha_1\}$ for the $\{j_1 j_2 j_3\}$ quantum numbers. The symbol $|0\rangle$ defines the model vacuum. $\{N\}$ specifies the norm, and the $\{\chi\}$'s denote the mode amplitudes. The superscript $\{1\}$ in the N's and $\{\chi\}$'s, as well as the subscript $\{1\}$ of the A's, characterize the excitation of one particle-hole pair.

If the quantum numbers of the valence-hole $\{j_1\}$ are not equal to the quantum numbers of the core-hole $\{j_3\}$, the set of states [Eq. (2.1)] is orthonormal, otherwise not. In the latter case the states are normalized via the orthogonalization procedure of Schmidt [17], which consists in evaluating the overlap integrals between the two nonorthogonal $A_1[j_1(j_2j_1)J_1;j]$ and $A_1[j_1(j_2j_1)J_1';j]$ states. With these integrals we define the orthogonal states as linear combination of the form

$$\Phi_{j-m}^1(\alpha_1 J_1)|0\rangle = \frac{1}{N}[\Phi_{j-m}^1(\alpha_1 J_1) - \langle A_1^\dagger(\alpha_1 J_1)|A_1(\alpha_1 J_1')\rangle \phi_{j-m}^1(\alpha_1 J_1')]|0\rangle.$$

The amplitudes of the different modes ($\chi_{\alpha_0 j}^0$ and $\chi_{\alpha_1 J_1 j}^1$) are calculated in the dynamic approximation of Ref. [6]. This approximation consists in evaluating the chain of commutators

$$[H,A_0(\alpha_0;j)] = \sum_{\alpha_0'} \varepsilon_j A_0(\alpha_0';j) + \sum_{\alpha_1 J_1} \langle A_0^\dagger(\alpha_0;j)\|V\|A_1(\alpha_1 J_1;j)\rangle A_1(\alpha_1 J_1;j), \qquad (2.2)$$

$$[H,A_1(\alpha_1 J_1;j)] = \sum_{\alpha_0'} \langle A_1^\dagger(\alpha_1 J_1;j)\|V\|A_0(\alpha_0';j)\rangle A_0(\alpha_0';j) + \sum_{\alpha_1' J_1'} \langle A_1^\dagger(\alpha_1 J_1;j)\|H\|A_1(\alpha_1' J_1';j)\rangle A_1(\alpha_1' J_1';j)$$

$$+ \sum_{\alpha_2'' J_1'' J_2''} \langle A_1^\dagger(\alpha_1 J_1;j)\|V\|A_2(\alpha_2'' J_1'' J_2'';j)\rangle A_2(\alpha_2'' J_1'' J_2'';j) \qquad (2.3)$$

and linearizing the $A_2(\alpha_2'' J_1'' J_2'';j)$ (3p-2p) terms in order to obtain, in the first-order linearization approximation, the eigenvalue equation for the $\{\chi\}$ amplitudes of the mixed model space $[1h$-$(2h$-$1p)]$

$$\chi_j^0 = \langle \Phi_0(A)|a_{jm}^\dagger|\Phi_h(A-1)\rangle,$$

$$\chi_{j_1(j_2j_3)J_1 j}^1 = \langle \Phi_0(A)|A_1^\dagger(j_1(j_2j_3)J_1)|\Phi_{2h1p}^1(A-1)\rangle.$$

In Eqs. (2.2) and (2.3) the nuclear Hamiltonian is

$$H = \sum_\alpha \varepsilon_\alpha a_\alpha^\dagger a_\alpha + \frac{1}{2} \sum_{\alpha\beta\gamma\delta} V_{\alpha\beta\gamma\delta} a_\alpha^\dagger a_\beta^\dagger a_\delta a_\gamma = H_0 + V,$$

where $V_{\alpha\beta\gamma\delta}$ are the matrix elements of the two-body potential V

$$V_{\alpha\beta\gamma\delta} = (\alpha\beta|V|\gamma\delta),$$

and ε_α are the single-particle energies. These can be calculated either in the HF approximation or, as assumed in this work, taken from the low-lying spectrum of neighboring closed-shell nuclei. The single-particle wave functions used to calculate the matrix elements of the two-body potentials

have been approximated by harmonic oscillator wave functions and the two-body potential has been assumed to have the form

$$V = e^{-(r/b)^2} \sum_{S,T} V_{ST} P_{ST},$$

where P_{ST} are the projection operators of the two-body states with quantum numbers S and T and where the parameters V_{ST} are discussed in Sec. IV. To calculate the matrix elements of the two-body interaction in Eqs. (2.2) and (2.3) we use the recoupling algebra of Ref. [18].

We obtain the following terms: (i) Single-hole energy, which can be calculated in the HF approximation or, as done in this work, taken from the spectrum of neighboring closed-shell nuclei, (ii) off-diagonal terms

$$= \sum_{J_i} (-1)^{j+j_2+J_i+J_1}(2J_i+1) \sqrt{\frac{2J_1+1}{2j+1}} \begin{Bmatrix} j & j_3 & J_i \\ j_2 & j_1 & J_1 \end{Bmatrix}$$

$$\times \langle jj_3|V|j_1j_2\rangle_{J_i}^a, \qquad (2.4)$$

(iii) diagonal terms

$$= \sum_{J_i} (-1)^{J_i+j_3'+j_2}(2J_i+1) \begin{Bmatrix} j_3 & j_2' & J_i \\ j_3' & j_2 & J_1 \end{Bmatrix} \langle j_3 j_2'|V|j_2 j_3'\rangle_{J_i}^a \delta_{J_1 J_1'}$$

$$+ \sum_{J_i} (2J_i+1)\sqrt{(2J_1+1)(2J_1'+1)} \begin{Bmatrix} j_2 & j_3 & J_1 \\ j_1 & j & J_i \end{Bmatrix}$$

$$\times \begin{Bmatrix} j_2 & j_3' & J_1' \\ j_1' & j & J_i \end{Bmatrix} \langle j_1' j_3'|V|j_1 j_3\rangle_{J_i}^a + \sum_{J_r J_i} (-1)^{j_1+j_3+J_1+J_1'}(2J_i+1)(2J_r+1)\sqrt{(2J_1+1)(2J_1'+1)} \begin{Bmatrix} J_1 & j_1 & j \\ j_2 & J_1' & J_r \end{Bmatrix}$$

$$\times \begin{Bmatrix} j_3 & j_2' & j_1 \\ j_3' & j_2 & J_r \end{Bmatrix} \begin{Bmatrix} j_3 & j_2' & j_1 \\ j_3' & j_2 & J_r \end{Bmatrix} \begin{Bmatrix} J_1 & j_3 & j_2' \\ j_3' & J_1' & J_r \end{Bmatrix} \langle j_2' j_1|V|j_2 j_3'\rangle_{J_i}^a$$

$$+ \sum_{J_r J_i} (-1)^{j_1'+j_2'+j_3+j}(2J_i+1)(2J_r+1)\sqrt{(2J_1+1)(2J_1'+1)} \begin{Bmatrix} J_1 & j_2' & j_3 \\ j_2 & J_1' & J_r \end{Bmatrix} \begin{Bmatrix} j_2 & j_1' & J_i \\ j_1 & j_2' & J_r \end{Bmatrix} \begin{Bmatrix} J_1 & j_1 & j \\ j_1' & J_1' & J_r \end{Bmatrix} \langle j_2 j_1'|V|j_1 j_2'\rangle_{J_i}^a$$

$$+ \sum_{J_i} (-1)^{j_1+j_1'+J_1+J_1'}(2J_i+1)\sqrt{(2J_1+1)(2J_1'+1)} \begin{Bmatrix} j_3 & j_2 & J_1 \\ j_1 & j_2' & J_i \end{Bmatrix} \begin{Bmatrix} j & j_1' & J_1' \\ j_2' & j_1 & J_1 \end{Bmatrix} \langle j_2' j_3|V|j_2 j_1'\rangle_{J_i}^a. \tag{2.5}$$

In Eqs. (2.4) and (2.5) $\begin{Bmatrix} a & b & c \\ d & e & f \end{Bmatrix}$ denotes the 6-J symbols as defined in Ref. [18] and the $\langle j_a j_b|V|j_c j_d\rangle_{J_i}^a$ are the antisymmetrized two-body matrix elements

$$\langle j_a j_b|V|j_c j_d\rangle_{J_i}^a = \langle [j_a j_b]^{J_i}|V|[j_c j_d]^{J_i} - [j_d j_c]^{J_i}\rangle.$$

Taking the expectation value of Eqs. (2.2) and (2.3) between the vacuum and the states $[|\phi_{j-m}(1h+2h1p)\rangle]^\dagger$ we obtain the eigenvalue equations that define the amplitudes $\chi_{\alpha_0 j}^0$ and $\chi_{\alpha_1 J_1 j}^1$ of the nuclear modes:

$$\sum_{\substack{j_1 j_2 j_3 \\ j_1' j_2' j_3'}} \begin{Vmatrix} E-\epsilon_j & V_{jj_3' j_1' j_2'} \\ V_{j_1 j_2 j j_3} & E-\epsilon_{j_i}+\epsilon_{j_2}-\epsilon_{j_3}+V_{j_1 j_2 j_3 j_1' j_2' j_3'} \end{Vmatrix} \begin{Vmatrix} \chi_{\alpha_0 j}^0 \\ \chi_{\alpha_1 J_1 j}^1 \end{Vmatrix} = 0. \tag{2.6}$$

Equation (2.6) is suitable to describe ground and excited states of the odd $(A-1)$ hole nuclei. The generalization of Eq. (2.6) to the isospin quantum numbers needed to describe the spectrum of light medium-mass nuclei has been described in Ref. [19]. For the ground state of ^{207}Pb with a $j=3p_{1/2}$ neutron hole, for the ground state of ^{165}Ho, Eq. (2.6), with a $j=2f_{7/2}$ proton hole, and for the ground state of the two Re isotopes with a $j=2d_{5/2}$ proton hole, the cutoff parameter is fixed at 24 MeV, so that the matrices we diagonalize are of the order of 1400×1400. The cutoff parameter has been introduced to limit the dimension of the eigenvalue matrix (2.6). Diagonalizing Eq. (2.6) we calculate the dynamic amplitudes of the ground-state modes. With these amplitudes we evaluate the reduced matrix elements of the operators O^λ that characterize the electromagnetic moments of order λ. Three terms contribute to the reduced transition-matrix elements in the DCM: (i) single-particle term

$$\equiv \chi_{\alpha_0 j}^0 \chi_{\alpha_0' j'}^0 (j\|O^\lambda\|j'), \tag{2.7}$$

(ii) off-diagonal terms

$$\equiv \chi_{\alpha_0 j}^0 \chi_{\alpha_1' J_1 j'}^1 \left[(-1)^{j_2'+j_3'}\sqrt{\frac{2j_1'+1}{2\lambda+1}}\,(j_3'\|O^\lambda\|j_2')\delta_{\lambda J_1'}\delta_{j_1' j} \right.$$
$$\left. +(-1)^{j_2'+j_1'}\cdot\sqrt{(2j_1'+1)(2J_1'+1)} \begin{Bmatrix} j & j_2' & J_1' \\ j_1' & j' & \lambda \end{Bmatrix} (j_2'\|O^\lambda\|j_1')\delta_{j_3' j} \right], \tag{2.8}$$

(iii) diagonal terms

$$
\begin{aligned}
&= \chi^1_{\alpha_1 J_1 j} \chi^1_{\alpha'_1 J'_1 j'} \sqrt{(2j+1)(2j'+1)(2J_1+1)(2J'_1+1)} \Bigg[(-1)^{j'_2+J_1+J'_1+j} \begin{Bmatrix} j'_2 & j_2 & \lambda \\ j'_1 & J_1 & j \\ J'_1 & j_3 & j' \end{Bmatrix} (j'_2\|O^\lambda\|j_2) \\
&+ (-1)^{j_2+j_3+j'_1+j} \begin{Bmatrix} J'_1 & j'_2 & j_3 \\ j_2 & J_1 & \lambda \end{Bmatrix} \begin{Bmatrix} J'_1 & j' & j'_1 \\ j & J_1 & \lambda \end{Bmatrix} (j'_2\|O^\lambda\|j_2) + (-1)^{j'_1+j_2+j_3+j'+J_1+J'_1} \begin{Bmatrix} j'_3 & J'_1 & j_2 \\ J_1 & j_3 & \lambda \end{Bmatrix} \\
&\times \begin{Bmatrix} J'_1 & j' & j'_1 \\ j & J_1 & \lambda \end{Bmatrix} (j_3\|O^\lambda\|j'_3) + \frac{(-1)^{J_1+j'_1+j+\lambda}}{\sqrt{(2J_1+1)(2J'_1+1)}} \begin{Bmatrix} j' & j'_1 & J_1 \\ j_1 & j & \lambda \end{Bmatrix} (j_1\|O^\lambda\|j'_1) + (-1)^{j'_3+j+J_1+\lambda} \\
&\times \begin{Bmatrix} j'_3 & j_2 & J'_1 \\ j_3 & j & J_1 \end{Bmatrix} \begin{Bmatrix} J_1 & j & j'_1 \\ \lambda & j'_3 & j' \end{Bmatrix} (j_1\|O^\lambda\|j'_3) + (-1)^{j'_1+j+J'_1+\lambda} \begin{Bmatrix} j_3 & j_2 & J_1 \\ j_1 & j & J'_1 \end{Bmatrix} \begin{Bmatrix} J'_1 & j' & j'_1 \\ \lambda & j_3 & j \end{Bmatrix} (j_3\|O^\lambda\|j'_1) \Bigg].
\end{aligned}
\tag{2.9}
$$

In Eqs. (2.7), (2.8), and (2.9) the operator O^λ successively represents the magnetic moment, the quadrupole moment, the hyperfine splitting (detailed structure of this operator is given in the next section), and the magnetic- and electric-distribution operators:

$$
\begin{Bmatrix} a & b & c \\ d & e & f \\ g & h & i \end{Bmatrix}
$$

is the 9J symbol, and the reduced matrix elements are defined according to Ref. [18]. If the operator O^λ represents the magnetic-moment operator $\Sigma_{\alpha\beta}(\alpha|g_l l_z + g_s s_z|\beta)a^\dagger_\alpha a_\beta$, the reduced matrix element on the right-hand side of Eq. (2.7) is the single-particle magnetic moment (Schmidt value). Although the corrections to the magnetic moments given by the right-hand side of Eq. (2.8) were already considered without the antisymmetrization effect in Ref. [2], the terms of the right-hand side of Eq. (2.9) represent something new, typical of nonperturbative dynamic-correlation theories. Unlike the calculations done in the perturbation theories, the right-hand side of Eq. (2.8) takes the antisymmetrization effect properly into account. Furthermore, the terms of Eq. (2.9) have been included exactly in the present calculations. They contribute coherently to the distribution of magnetization in nuclei. In a
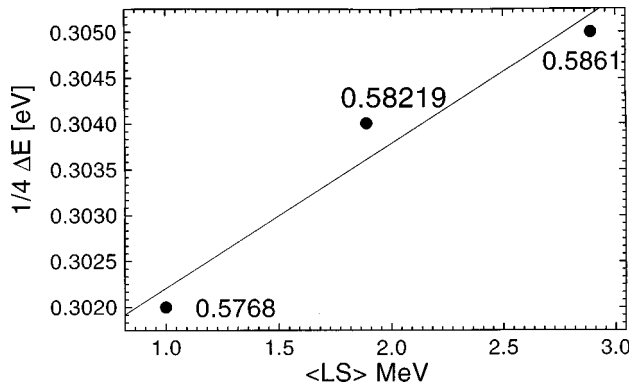

FIG. 1. Dependence of the hyperfine splitting on the (LS) strength parameter for ^{207}Pb. The dots give the respective magnetic moments.

perturbative approximation these terms are proportional to the second-order diagrams of the theory if we neglect the Pauli-antisymmetrization principle. This comparison between our calculation and the perturbative calculation is to be considered formal, because, due to diagonalization method and to the large number of components introduced, the CMW functions of the DCM describes the collective modes of the nucleus, an effect that cannot be found in perturbative calculations.

III. INTERACTION WITH THE ATOMIC MAGNETIC FIELD

Exotic atoms, i.e., atoms with configurations deviating strongly from conditions typically realized in nature, offer fascinating possibilities for testing nuclear models. Such ex-

TABLE I. List of the three terms that in the DCM contribute to the hypefine splitting. The single particles have to be associated to $\{\epsilon\}$ of Ref. [14]. The terms $\Delta E_{\text{off-diag}}$ have been introduced accordingly Ref. [22]. ΔE_{diag} has been not considered by the other theories.

^{165}Ho^{66+}	$\Delta E_{\text{sp}}=$	2.16910
	$\Delta E_{\text{off-diag}}=$	0.01667
	$\Delta E_{\text{diag}}=$	-0.02137
	Total	2.16490
^{185}Re^{74+}	$\Delta E_{\text{sp}}=$	2.7591
	$\Delta E_{\text{off-diag}}=$	0.0189
	$\Delta E_{\text{diag}}=$	-0.0580
	Total	2.7192
^{187}Re^{74+}	$\Delta E_{\text{sp}}=$	2.7839
	$\Delta E_{\text{off-diag}}=$	0.0349
	$\Delta E_{\text{diag}}=$	-0.0730
	Total	2.7449
^{207}Pb^{81+}	$\Delta E_{\text{sp}}=$	1.20021
	$\Delta E_{\text{off-diag}}=$	0.03578
	$\Delta E_{\text{diag}}=$	-0.01879
	Total	1.21660

TABLE II. The different contributions to the hyperfine splitting.

	$^{209}\text{Bi}^{82+}$	$^{207}\text{Pb}^{81+}$	$^{165}\text{Ho}^{66+}$	$^{185}\text{Re}^{74+}$	$^{187}\text{Re}^{74+}$
rms radius	5.519 fm	5.497 fm	5.21 fm	5.37 fm	5.37 fm
Magnetic moment (corrected) [29]	$4.1106(5)\mu_N$	$0.58219()\mu_N$	$4.132(3)\mu_N$	$3.1871(3)\mu_N$	$3.2197(3)\mu_N$
Point nucleus (Dirac) [10,15]	212.320 nm	885.76 nm	538.90 nm	411.87 nm	407.70 nm
+ Breit-schawlow	238.791(50) nm	989.66(1) nm	564.67 nm	443.18 nm	438.68 nm
+ DCM contribution	243.91(38) nm	1019.1(1.6) nm	572.6 nm	455.78 nm	451.53 nm
Vacuum Polarization [10]	−1.64 nm	−6.83 nm	−2.46 nm	−2.44 nm	−2.40 nm
Self-energy [15]	2.86 nm	11.9 nm	5.20 nm	4.76 nm	4.66 nm
Total QED [15]	1.22 nm	5.08 nm	2.72 nm	2.31 nm	2.26 nm
Theory incl. QED	245.13(58) nm	1024.2(2.0) nm	575.32 nm	458.11 nm	453.79 nm
Experiment	243.87(2) nm(1)	1019.7(2) nm	572.79(15) nm	456.05(30) nm	451.69(30) nm

otic atoms exhibit the interplay of nuclear and atomic quantities. They permit one to test specific parts of the electromagnetic interaction by selectively changing or observing the effect of just a single parameter much as precise studies have been made in the past using muonic atoms [20].

It is now possible to produce a wide variety of exotic atoms from energetic heavy-ion collisions. For example, hydrogenlike high-Z atoms such as the ones considered in the present investigation have recently become available for experiments at Darmstadt [11] and Livermore [12,13]. In Darmstadt at GSI ^{207}Pb has been produced from heavy ions accelerated to several hundred MeV/nucleon at the SIS accelerator. Because they are then stored and cooled in the ESR storage ring, they can be studied without the usual constraints of unsatisfactory accelerator-beam quality and short observation time. Where previously only the ground-state hyperfine structure (HFS) splitting in muonic ^{209}Bi could be studied, it is now possible to investigate the corresponding electronic effects in the hydrogenlike Pb ions.

Because the HFS splitting is proportional to Z^3, the wave length of the $M1$ transition between the ground-state components of hydrogenlike ions with high Z is in the optical regime. This is dramatically different from the case of hydrogen where the 21-cm radiation of the HFS splitting is in the microwave regime. As a result it was possible to measure the ground-state HFS splitting of hydrogenlike ^{207}Pb by laser-induced fluorescence spectroscopy [11]. The experiment yielded a ground-state energy splitting of $\Delta E^{\text{exp}} = 1.216$ (1) eV and achieved a relative accuracy of $\simeq 10^{-4}$. This high accuracy has made possible the first test of QED in the strong magnetic field of the highly charged heavy ion.

At Livermore hydrogenlike ^{165}Ho, ^{185}Re, and ^{187}Re have been produced and stored in a high-energy electron-beam ion trap (Super EBIT) [12,13] by a variable-energy electron beam axially compressed by a high magnetic field. The Livermore experiments yielded ground-state-energy splittings of 2.1646(3) eV for ^{165}Ho, 2.7187(18) eV for ^{185}Re, and 2.7449(18) eV for ^{186}Re.

The aim of the present calculations is to compare the theoretical hyperfine splittings obtained in the DCM to the ones obtained in the single-particle approximation [15] and to the experimental values. In order to calculate the hyperfine splitting in the DCM we need precise information about both the nuclear and the electron wave functions.

The nuclear wave functions are calculated as in Sec. II. With these wave functions the calculated basic properties of the ground states of the nuclei under investigation are in good agreement with the experimentally determined values.

The electron is described as a Dirac particle moving in the Coulomb potential generated by a charge distribution of a Fermi type. To solve the Dirac equation we have approximated the nuclear density distribution with a two-parameter Fermi distribution as de Vries et al. [21] did. The magnetic interaction of the electron with charge of the nucleus is given by

$$V^{e-N} = e \int d^3\vec{r}_e \psi_e^*(\vec{r}_e)\, \vec{\alpha}\cdot\vec{A}(\vec{r}_e)\, \psi_e(\vec{r}_e),$$

where

$$\vec{A}(\vec{r}_e) = -\int d^3\vec{r}_j \vec{m}(\vec{r}_j)\times\vec{\nabla}_e \frac{1}{|\vec{r}_e-\vec{r}_j|}$$

with

$$\vec{m}(\vec{r}_j) = \mu_0 \sum_i (g_l^i \vec{l}_i + g_s^i \vec{s}_i)\, \delta(\vec{r}_j - \vec{r}_i).$$

From these expressions, making a multipole-expansion of $\vec{A}(\vec{x})$ and using some recoupling, we obtain

$$\Delta E = C(A_L + A_S) \tag{3.1}$$

with

$$C = \frac{F(F+1)-I(I+1)-j(j+1)}{2Ij}\bigg|_{F_1}^{F_2},$$

where F designates the total−angular=momentum quantum number of the electron-nucleus system. I is the angular mo-
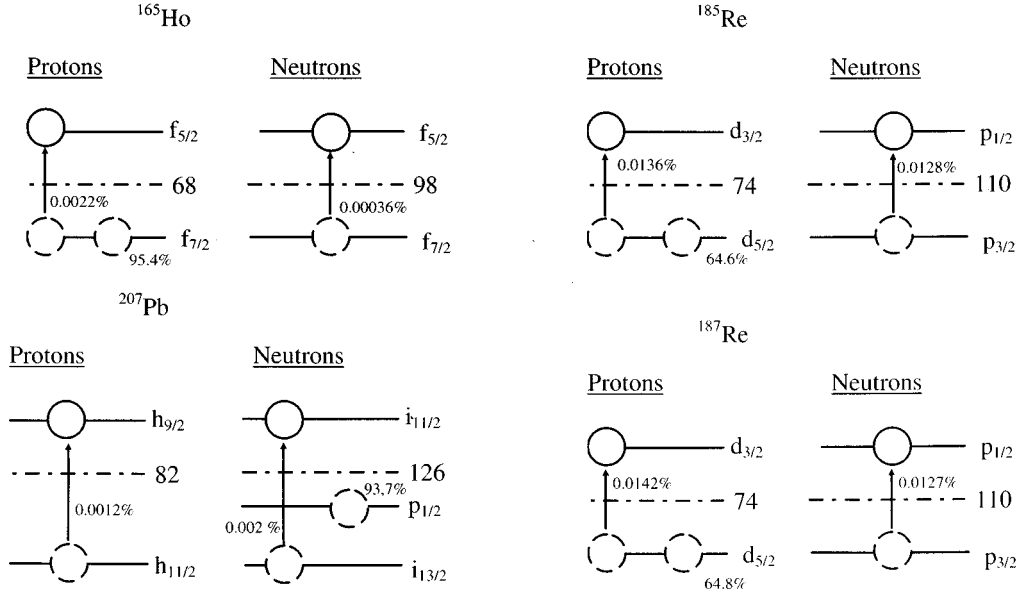
FIG. 2. The square of the amplitude of the single-particle and of the terms corresponding to the first-order contributions calculated for the ground states of the four nuclei from the diagonalization of the eigenvalue Eq. (2.6).

mentum quantum number of the nucleus and j is the angular-momentum quantum number of the electron, so that $|F_1| \leq F \leq F_2$.

For ^{207}Pb we have $C_2 - C_1 = 4$, for ^{165}Ho $C_2 - C_1 = 2.8$, and for both Re isotopes $C_2 - C_1 = 2.4$. For ^{207}Pb this leads to the value

$$\Delta E = 4(A_L + A_S),$$

for ^{165}Ho to the value

$$\Delta E = 2.28(A_L + A_S),$$

and for both Re isotopes to the value

$$\Delta E = 2.4(A_L + A_S).$$

TABLE III. Calculated rms radii, nuclear magnetic moments (mm), and nuclear quadrupole moments (QM) of ^{165}Ho, ^{185}Re, ^{187}Re, and ^{207}Pb ground states.

	$\langle r^2 \rangle^{1/2}$	MM	QM
^{165}Ho^{66+}			
th.	5.210 fm	4.132 nm	-0.35
exp.	5.210(7) fm [30]	4.132(3) nm [31]	
^{185}Re^{74+}			
th.	5.389 fm	3.1870 nm	0.15
exp.	5.391(1) fm [12]	3.1871(3) nm [31]	
^{187}Re^{74+}			
th.	5.395 fm	3.2196 nm	0.17
exp.	5.391(1) fm [12]	3.2197(3) nm [31]	
^{207}Pb^{81+}			
th.	5.496 fm	0.5820 nm	0
exp.	5.494(6) fm [30]	0.58219(2) nm [29]	

The A_L and A_S are the orbital-angular-momentum part and the spin-angular-momentum part, respectively. In the second quantization formulation these operators are given by

$$A_L = \frac{4}{3} e \mu_N \left\langle \phi_{j-m} \left| \sum_{\alpha\beta} (\alpha|O_L|\beta) a_\alpha^\dagger a_\beta \right| \phi_{j-m} \right\rangle, \quad (3.2)$$

and

$$A_S = \frac{4}{3} e \mu_N \left\langle \phi_{j-m} \left| \sum_{\alpha\beta} (\alpha|O_S|\beta) a_\alpha^\dagger a_\beta \right| \phi_{j-m} \right\rangle, \quad (3.3)$$

where

$$O_L = g_l l_z \left[\int_R^\infty f(r)g(r) dr + \int_0^R \left(\frac{r}{R}\right)^3 f(r)g(r) dr \right] \quad (3.4)$$

and

$$O_S = g_s s_z \int_R^\infty f(r)g(r) dr - \sqrt{\frac{\pi}{2}} [Y_2 \otimes \sigma]^1$$

$$\times \int_0^R \left(\frac{r}{R}\right)^3 f(r)g(r) dr. \quad (3.5)$$

In Eqs. (3.3)–(3.5) μ_0 is the nuclear magneton, g_l and g_s are the orbital and spin g factors, the notation $[Y_2 \otimes \sigma]^1$ means the coupling of Y_2 with the nucleon spin operator σ to a spherical tensor of rank one, f and g are the Dirac spinors, and $\{\phi_{j-m}\}$ is the ground-state wave function [see Eq. (2.1)]. The latter term with $[Y_2 \otimes \sigma]^1$ is the asymmetry term of Bohr [14]. Using the ground-state wave function of Eq. (2.1) we obtain the following contributions to the hyperfine splitting;

$$\Delta E = C(\Delta E_{sp} + \Delta E_{off\text{-}diag} + \Delta E_{diag}). \quad (3.6)$$

The term ΔE_{sp} is given by Eq. (2.7), the term $\Delta E_{off\text{-}diag}$ by Eq. (2.8), and the term ΔE_{diag} by the Eq. (2.9). The single-
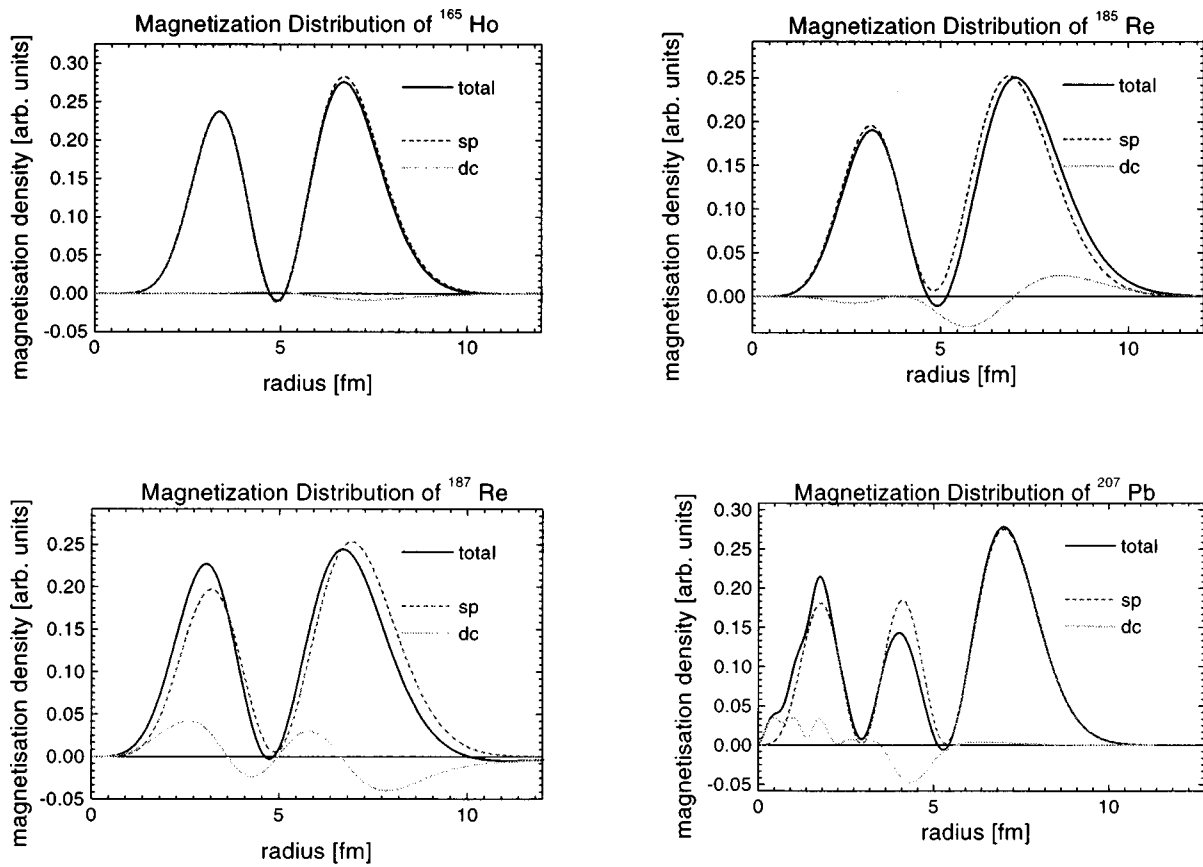
FIG. 3. The normalized magnetization distribution (full line) given in terms of the single particle (dashed line) and dynamic-correlation (dot line) contributions as a function of the radial coordinate.
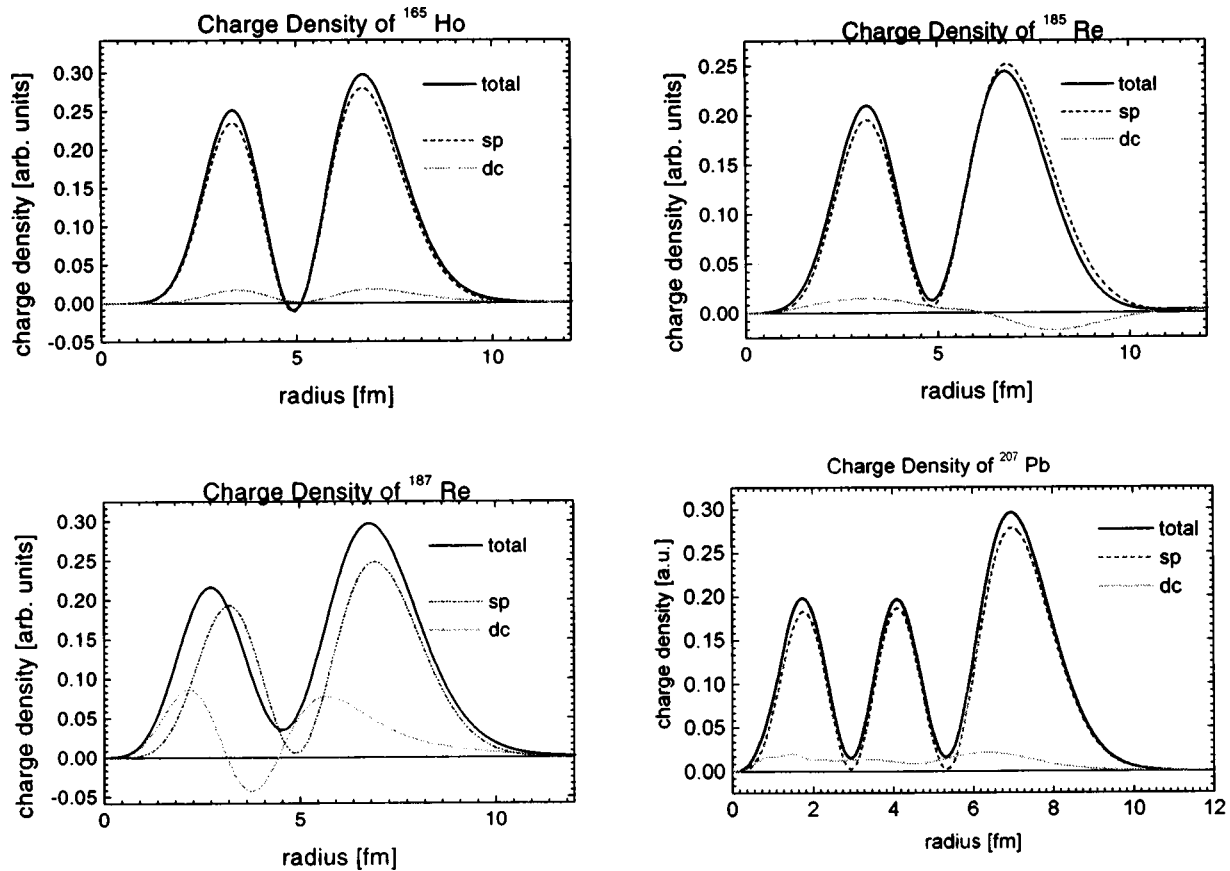
FIG. 4. The normalized charge distributions (full line) given in terms of the single particle (dashed line) and dynamic-correlation (dot line) contributions as a function of the radial coordinate.

particle term includes implicitly the Bohr-asymmetry term of Ref. [14]. The off-diagonal term is proportional to the term obtained by a nonperturbative calculation as described in Ref. [22]. The DCM terms have not until now been analyzed. The results of the calculation of the hyperfine structure splitting are presented in Table I where the different contributions of Eq. (3.6) are given without the QED corrections. Note that in the DCM two additional terms appear to contribute to the hyperfine splitting. These terms have not been considered in the Bohr-Weisskopf {ϵ} of Ref. [14]. In Fig. 1 we give for ^{207}Pb the dependence of the hyperfine splitting on the spin-orbit force.

The hyperfine splitting as derived in the present nonlinear formulation Eq. (3.6) can be compared with the results of Refs. [14,15], where the hyperfine splitting is calculated from the formula

$$\Delta E(\mu) = \frac{4}{3} \alpha (\alpha Z)^3 \frac{\mu}{\mu_N} \frac{m}{m_N} \frac{2I+1}{2I} mc^2$$
$$\times \{A(\alpha Z)(1-\delta)(1-\varepsilon) + x_{\mathrm{rad}}\}. \quad (3.7)$$

Here α is the fine structure constant, Z is the nuclear charge, m is the electron mass, m_N is the proton (neutron) mass, μ is the nuclear magnetic moment, μ_N is the nuclear magneton, and I is the nuclear spin. The relativistic correction $A(\alpha Z)$ is obtained from exact solution of the Dirac equation with a Coulomb potential. The factor $(1-\delta)$ corrects for the finite spatial distribution of the nuclear charge (Breit-Schawlow correction), $(1-\epsilon)$ corrects for the finite spatial distribution of the nuclear magnetization and for the asymmetry term which results from coupling the valence particle with the core degrees of freedom (Bohr-Weisskopf correction [14]). x_{rad} stands for the QED corrections. The radiative corrections to order α have been calculated in the Ref. [15]. Since this effect yields ΔE^{VP} or $\Delta \lambda$, the importance of determining the self-energy part of the radiative corrections in order to explain theoretically the experimental value is evident. In the extreme single-particle model QED and nuclear-magnetization corrections for high-Z atoms are of the same order of magnitude. Therefore the feasibility of testing the QED corrections depends strongly on the accuracy of the model used to evaluate the effects of nuclear magnetization. The results of this perturbation calculations are presented in Table II where we have attributed, as in Ref. [1], the Bohr-Weisskopf effect to the three terms of Table I. The theoretical calculations reproduce the experimental HFS splitting if the QED corrections are neglected. However, from the analysis done in this work, the Bohr-Weisskopf effect has to be attributed only with the single-particle term of the DCM. A numerical comparison of the single-particle contribution with the results of Ref. [15] is in favor of this assumption. The new analysis presented in Ref. [23], which assumes for ^{207}Pb a larger magnetic moment, is giving, to our opinion, a too large Bohr-Weiskopf contribution, by overestimating the asymmetry terms. The other two terms of Table I contribute to the HFS splitting proportionally to the QED corrections (the values given in Table II for ^{165}Ho^{66+}, ^{185}Re^{74+}, ^{187}Re^{74+}, ^{207}Pb^{81+}, and ^{209}Bi^{82+} were obtained from Ref. [15]).

To conclude we note the following.

(a) Perturbation approximations given by Eq. (3.7) assume that the global contributions to the hyperfine splitting are attributed to a point nucleus approximation. In this approximation the nuclear magnetic moment is a well defined input. The nuclear effects are included as a small perturbation {ϵ}. The radiative corrections x_{rad} are then calculated according to QED perturbation theory.

(b) The nonperturbative calculation does not modify the structure of the single-particle (hole) operators but calculates the effective operators directly from the configuration space.

The terms $\Delta E_{\mathrm{off\text{-}diag}}$ and ΔE_{diag} are typical of a dynamic theory and are very important to give a good theoretical description of the magnetic structure of the nucleus. Since we have included in the theory meson effects, we would expect that DCM contributions to the hyperfine splitting are proportional to the diagrams of the QED perturbation theory. The advantages of DCM calculations relative to perturbative theories are that we do not need to modify the gyromagnetic factors of the magnetic operators and that the three terms which contribute to the hyperfine splitting arise from the same model.

IV. NUCLEAR PARAMETERS

To calculate the electromagnetic properties of the ground states of the ^{165}Ho, ^{185}Re, ^{186}Re, and ^{207}Pb nuclei, we have to make, as in the case of ^{209}Bi, some assumptions about the input parameters of the theory, i.e., single-particle wave functions, single-particle energy, and two-body potentials. The following single-particle configuration space has been used.

Proton hole: $2p_{3/2}$, $1f_{5/2}$, $2p_{1/2}$, $1g_{9/2}$, $2d_{5/2}$, $1g_{7/2}$, $3s_{1/2}$, $2d_{3/2}$, $1h_{11/2}$.

Proton particle: $1h_{9/2}$, $2f_{7/2}$, $3p_{3/2}$, $3p_{1/2}$, $1i_{13/2}$, $3d_{5/2}$, $2g_{7/2}$, $4s_{1/2}$, $3d_{3/2}$, $2h_{11/2}$.

Neutron hole: $2d_{5/2}$, $1g_{7/2}$, $3s_{1/2}$, $2d_{3/2}$, $1h_{11/2}$, $1h_{9/2}$, $2f_{7/2}$, $3p_{3/2}$, $2f_{5/2}$, $3p_{1/2}$, $1i_{13/2}$.

Neutron particle: $3d_{5/2}$, $2g_{7/2}$, $4s_{1/2}$, $3d_{3/2}$, $2h_{11/2}$, $1j_{15/2}$, $1i_{11/2}$, $2g_{9/2}$.

The single-particle energies are those of Kuo [24]. The single-particle wave functions are assumed to be harmonic-oscillator wave functions with size parameters chosen to reproduce Wood-Saxon wave functions as proposed in Ref. [25].

In Eqs. (2.5) two types of two-body matrix elements occur: (1) particle-hole matrix elements and (2) hole-hole matrix elements. The two-body model potential used to calculate the particle-hole matrix elements (1) is taken from Ref. [25] (V_{ST} of COP type) while the two-body model potential used to calculate the hole-hole matrix elements (2) is taken from Ref. [26]. The matrix elements of Eq. (2.4) are of mixed type and are calculated from hole-hole potential. The strength of this force is weakened in comparison with the one used for the $(A+1)$ nuclei. The particle-hole potential already has been successfully applied in the theoretical description of the septuplet states in ^{209}Bi (see Ref. [27]), while the V_{ST} parameters of the particle-particle potential have been derived by fitting the two-body matrix elements calculated with the Bethe-Goldstone formalism as described in Ref. [26]. The depth of the particle-hole potential is chosen to reproduce the energy of the first 3^- state in ^{208}Pb. The

particle-particle potential has been adjusted to reproduce the level scheme of ^{210}Bi [28] and to calculate the spectrum of the excited states in ^{209}Bi as preliminarily shown in Ref. [27].

With these parameters, diagonalizing Eq. (2.6) for $\{j^\pi = 7/2^-, 5/2^+, 1/2^-\}$ we obtain the wave functions of the DCM. In Fig. 2 we give the spin-flip 1^+ amplitudes calculated for the different nuclei. The remaining $(2h\text{-}1p)$ amplitudes, not given explicitly, are small compared to the 1^+ amplitudes but counteract the deviation produced in the magnetic structure by the first-order approximation. In Table III we compare the calculated nuclear magnetic moments, the nuclear quadrupole moments, and the nuclear rms radii for ^{165}Ho, ^{185}Re, ^{187}Re, and ^{207}Pb with the experimental quantities. The agreement between the experimental [21,29–32] and theoretical values is remarkably good. The small discrepancy between the computed nuclear radius and the experimentally quoted one is probably due to the $4h\text{-}3p$ components not included in the calculations (i.e., the CMWFs of the third kind which allow for the formation of low lying $\{0^+\}$ states). On the other hand, the calculated nuclear radii agree remarkably well with the results obtained in calculations done within the framework of a relativistic mean-field theory. In Fig. 3 we have plotted the normalized ground-state magnetization distributions. In Fig. 4 we give the normalized ground-state charge distributions.

V. DISCUSSION

This paper has used the DCM to analyze the structure of the hyperfine splittings of ^{207}Pb, ^{165}Ho, and ^{185,187}Re. These nuclei are characterized by one hole in the closed shell. It models these nuclei with nonperturbative equations of motion which introduce into the structure calculations of the $(A-1)$ nuclei and the $2h\text{-}1p$ and $3h\text{-}2p$ configurations. The model reproduces very well the magnetic moments of these $(A-1)$ isotopes. The distribution of magnetization calculated in this way differs from the normally assumed shape. In particular the distribution of the magnetic moment extends farther out than the charge distribution. In its consequence on the hyperfine splitting this is similar to the model proposed by Bohr and Weisskopf [14]. There the single-particle description of the nucleus has been refined by the addition of an asymmetry term which represents the interaction with the rotational flow of the reference nucleus. Compared to a single particle treatment, however, the results of DCM show a smaller variation between the nuclei studied here than the application of Bohr's prescription [14,15]. Three terms contribute to the theoretical energy splittings. The first term is due to the single hole, the second to diagrams that in the perturbative calculation are proportional to the term introduced by Le Bellac [22], and the third term characterizes the dynamics of the model. With these three terms the DCM calculations and experimental observations of HFS splitting of hydrogenlike Ho, Re, Pb, and Bi agree quite exactly as long as no QED corrections are added to the DCM calculations. This seems to be very significant in view of the different nuclear structure of these nuclei. Independent calculations of the size of the QED contributions result in values close to 0.5% for all these candidates. Inclusion of the QED effects introduces a discrepancy of that magnitude. This has led us to examine the DCM more closely again to see if it already includes the equivalent of the QED corrections. One could speculate that these corrections may be part of the non-normal parity states of core polarization that can be identified with low-energy mesons. Presently only the similar size of these contributions is in favor of such an argument. Another possible explanation for a deviation with slow variation along the table of isotopes might be an underrepresentation of specific contributions in the dynamic mixing prescription. A study of the sensitivity to details of the mixing procedure is under way using an RPA approach for the DCM.

[1] M. Tomaselli, S. M. Schneider, E. Kankeleit, and T. Kühl, Phys. Rev. C **51**, 2989 (1995).

[2] H. Noya, A. Arima, and H. Horie, Prog. Part. Nucl. Phys. **1**, 41 (1958).

[3] R. Bauer, J. Speth, V. Klemt, P. Ring, E. Werner, and T. Yamazaki, Nucl. Phys. **A209**, 535 (1973); T. Fujita and A. Arima, *ibid.* **A254**, 513 (1975); C. Mahaux, R. F. Bortignon, R. A. Broglia, and C. H. Dasso, Phys. Rev. **120**, 1 (1985).

[4] I. S. Towner, Prog. Part. Nucl. Phys. **11**, 1991 (1984); T. Ericson and W. Weise, *Pions and Nuclei* (Clarendon, Oxford, 1958).

[5] F. C. Khanna and O. Hausser, Phys. Lett. B **46**, 12 (1993).

[6] M. Tomaselli, Phys. Rev. C **37**, 343 (1988); Ann. Phys. (N.Y.) **205**, 362 (1991); Phys. Rev. C **48**, 2290 (1993).

[7] M. Tomaselli, D. Herold, and L. Grünbaum, Nuovo Cimento **46**, 1431 (1978).

[8] M. J. G. Borge, N. Cronberg, M. Cronqvist, H. Gabelmann, P. G. Hansen, L. Johannsen, B. Janson, S. Mattson, G. Nyman, A. Richter, and M. Tomaselli, Nucl. Phys. **A490**, 887 (1988).

[9] R. W. Hasse, B. L. Friman, and D. Berdichevsky, Phys. Lett. B **181**, 5 (1986); M. M. Sharma, G. A. Lalazissis, and P. Ring, *ibid.* **317**, 9 (1993); N. Tajima, P. Bonche, H. Flocard, P. H. Heenen, and M. S. Weiss, Nucl. Phys. **A551**, 434 (1993).

[10] M. Finkbeiner, B. Fricke, and T. Kühl, Phys. Lett. A **176**, 153 (1993); S. M. Schneider, J. Schaffner, W. Greiner, and G. Soff, J. Phys. B **26**, 581 (1993).

[11] I. Klaft, S. Borneis, T. Engel, B. Fricke, R. Grieser, G. Huber, T. Kühl, D. Marx, R. Neuman, S. Schröder, P. Seelig, and L. Völker, Phys. Rev. Lett. **73**, 2425 (1993); P. Seelig, S. Borneis, A. Dax, T. Engel, S. Faber, M. Gerlach, C. Holbrow, G. Huber, T. Kühl, D. Marx, K. Meier, P. Merz, W. Quint, F. Schmitt, M. Tomaselli, L. Völker, H. Winter, M. Würtz, K. Beckert, B. Franzke, F. Nolden, H. Reich, M. Steck, and T. Winkler, Phys. Rev. Lett. (to be published).

[12] J. R. Crespo Lopez-Urrutia, P. Beiersdorfer, B. B. Birkett, K. Widmann, A.-M. Mårtensson-Pendrill, and M. G. H. Gustavs-

son, Phys. Rev. Lett. **77**, 826 (1996).

[13] J. R. Crespo Lopez-Urrutia, P. Beiersdorfer, D. W. Savin, and K. Widmann, Phys. Rev. Lett. **77**, 826 (1996).

[14] A. Bohr and V. F. Weisskopf, Phys. Rev. **77**, 94 (1950); A. Bohr, *ibid.* **81**, 134 (1951).

[15] V. M. Shabaev, M. Tomaselli, T. K. Kühl, A. N. Artemyev, and V. A. Yeroklin, Phys. Rev. A **56**, 252 (1997); S. M. Schneider, J. Schaffner, W. Greiner, and G. Soff, J. Phys. B **26**, 118 (1994); S. M. Schneider, W. Greiner, and G. Soff, Phys. Rev. A **50**, 118 (1994); H. Person, S. M. Schneider, G. Soff, and W. Greiner, Phys. Rev. Lett. **76**, 1433 (1996).

[16] G. E. Brown, *Unified Theory of Nuclear Models* (North-Holland, Amsterdam, 1964).

[17] Morse and Feshbach, *Methods of Theoretical Physics* (McGraw-Hill, New York, 1953).

[18] G. Racah, CERN Report No. 61, 1961, p. 8; A. De-Shalit and I. Talmi, *Nuclear Shell Theory* (Academic, New York, 1963).

[19] M. Tomaselli and Herold (unpublished).

[20] A. Rüetschi, L. Schellenberg, T. Q. Phan, G. Piller, L. A. Schaller, and H. Schneuwly, Nucl. Phys. **A422**, 461 (1986); R. Bauer, J. Speth, V. Klemt, P. Ring, E. Werner, and T. Yamazaki, *ibid.* **A209**, 535 (1973); H. Backe, R. Engfer, E.

Kankeleit, R. Link, R. Michaelsen, C. Petitjean, H. Schneuwly, W. V. Schroeder, J. L. Vuilleumier, H. K. Walter, and A. Zehnder, *ibid.* **A234**, 469 (1979).

[21] H. de Vries, C. W. de Jager, and C. de Vriex, At. Data Nucl. Data Tables **36**, 495 (1987).

[22] M. Le Bellac, Nucl. Phys. **40**, 645 (1963).

[23] V. M. Shabaev, M. B. Shabaeva, I. I. Tupitsyn, and V. A. Yerokhin, Hyperfine Interact. (to be published).

[24] T. T. S. Kuo and G. H. Herling, Report No. NRL2258, Washington, DC, 1971 (unpublished); (private communication).

[25] V. Gillet, A. M. Green, and E. A. Sanderson, Nucl. Phys. **88**, 321 (1966).

[26] Y. E. Kim and J. O. Rasmussen, Nucl. Phys. **47**, 184 (1963).

[27] M. Tomaselli and D. Herold (private communication).

[28] W. Y. Lee *et al.*, Nucl. Phys. **A181**, 16 (1972).

[29] E. W. Otten, *Nuclear Radii and Moments of Unstable Nuclei*, edited by D. A. Bromley, (Plenum, New York, 1988), Vol. 7, pp. 515.

[30] P. Raghavan, At. Data Nucl. Data Tables **42**, 189 (1989).

[31] I. Angeli and M. Csatlós, Atomiki Közlemények **20**, 1 (1978).

[32] R. Firestone *et al.*, *Table of Isotopes*, edited by V.S. Shirley (Wiley, New York, 1996), Appendix E.